

Inelastic lateral-distortional buckling of continuously restrained rolled I-beams

Dong-Sik Lee[†]

Earthquake Engineering Research Center, Seoul National University, Seoul 151-744, Korea

Mark A. Bradford[‡]

*School of Civil and Environmental Engineering,
The University of New South Wales, UNSW, Sydney, NSW 2052, Australia*

(Received February 25, 2002, Revised July 11, 2002, Accepted August 1, 2002)

Abstract. An energy method of analysis is presented which can be used to study the inelastic lateral-distortional buckling of hot-rolled I-sections continuously restrained at the level of the tension flange. The numerical modelling leads to the incremental and iterative solution of a fourth-order eigenproblem, with very rapid solutions being obtainable, so as to enable a study of the factors that influence the strength of continuously restrained I-beams to be made. Although hot-rolled I-sections generally have stocky webs and are not susceptible to reductions in their overall buckling loads as a result of cross-sectional distortion, the effect of elastic restraints, particularly against twist rotation, can lead to buckling modes in which the effect of distortion is quite severe. While the phenomenon has been studied previously for elastic lateral-distortional buckling, it is extended in this paper to include the constitutive relationship characteristics of mild steel, and incorporates both the so-called 'polynomial' and 'simplified' models of residual stresses. The method is validated against inelastic lateral-torsional buckling solutions reported in previous studies, and is applied to illustrate some inelastic buckling problems. It is noted that over a certain range of member slenderness the provisions of the Australian AS4100 steel standard are unconservative.

Key words: beams; continuous restraint; elastic restraint; energy method; inelastic buckling; residual stresses; yielding.

1. Introduction

The concept of lateral-distortional buckling in I-section beams is well-known (Bradford 1992). Almost all studies have been restricted to elastic buckling, where the lateral-torsional and lateral-distortional buckling loads of practical I-beams are almost identical if the beam is simply supported without restraint along its length. This is not the case for beams with incomplete end restraint (Bradford and Trahair 1981, 1983, Bradford 1990), or for beams with continuous elastic restraint of the tension flange (Bradford 1988a). The latter case of beam restraint is often met in practice, such as in a half-through girder bridge, with a standing-seam sheeting system, and in a composite bridge girder near an

[†]Post-doctoral Research Fellow

[‡]Professor

internal support or in a composite beam-to-column connection in a building. This paper aims to extend the energy-based method of elastic distortional buckling of continuously restrained I-beams into the inelastic domain, and includes residual stresses in addition to the standard elastic-plastic-strain hardening idealisation of the stress-strain law for mild steel.

Research into the inelastic lateral-torsional buckling of unrestrained I-section members subjected to uniform bending has been reasonably plentiful. Ketter *et al.* (1955) developed a simplified residual stress model, and applied it to members subjected to unequal end moments with axial thrust. Galambos (1963) also considered this problem, which was refined in the accurate modelling developed by Trahair and Kitipornchai (1972) and Kitipornchai and Trahair (1975), and in the finite element study of Nethercot (1974). Some other studies of inelastic lateral-torsional buckling are reviewed in Trahair (1993). The inelastic lateral-distortional buckling of beams under uniform bending was investigated by Bradford (1988b), but the cross-section considered was assumed to be fabricated from very slender plates, and consequently residual stresses germane to fabrication by welding were assumed.

This paper considers the inelastic lateral-distortional buckling of hot-rolled I-section beams subjected to uniform bending, but which may also be restrained elastically by a continuous restraint against lateral deflection, in-plane rotation and twist rotation at the level of the tension flange. Trahair and Kitipornchai (1972) showed that the inelastic buckling study of beams with undeformable cross-sections may be undertaken by assuming that the cross-section is monosymmetric, owing to the combination of yielding and residual stresses under monotonically increasing end moments, and used the elastic modulus E in the elastic region and the strain hardening modulus E_{st} in the yielded regions. In addition, since the bending moment and residual stresses do not vary along the member, the monosymmetric idealisation is also prismatic. This paper, however, differs from Kitipornchai and Trahair's work in that the cross-section may distort, requiring four degrees of freedom instead of two to model the buckling mode at each section along the beam. The flexible web is analysed using an inelastic plate buckling model, while the effects of continuous elastic restraints, which do not appear to have been treated hitherto in the literature, are included.

2. Theory

2.1. General

The energy method used by Bradford (1988a) for elastic distortional buckling forms the basis of the analysis herein. The member is assumed to be a doubly-symmetric hot-rolled I-section beam, simply supported at the ends and acted upon by equal and opposite end moments that bend the member into single curvature. While this formulation restricts the loading to comprise of uniform stress longitudinally and the end conditions to be those of simple supports, it is intended to shed light using an efficient algorithm on the cross-section geometric and elastic restraint stiffness parameters that affect the buckling strength. The residual stresses induced during the cooling of a hot rolled member are usually described by the polynomial model (Fig. 1a) or by the simplified model (Fig. 1b), descriptions of which are given elsewhere (Lee and Bradford 2002). During buckling, the stocky flanges are assumed to remain rigid, and their buckling is therefore treated as that of rigid bars. On the other hand, the web is assumed to buckle as a cubic curve, for which plate theory is invoked. The beam of length L is shown in Fig. 2a, with the moments in Fig. 2b. An arbitrary reference axis is positioned along the beam at the web mid-height. The concept of the arbitrary reference axis was explained by Bradford and Cuk (1988), where the derivations in their finite element buckling model of elastic monosymmetric

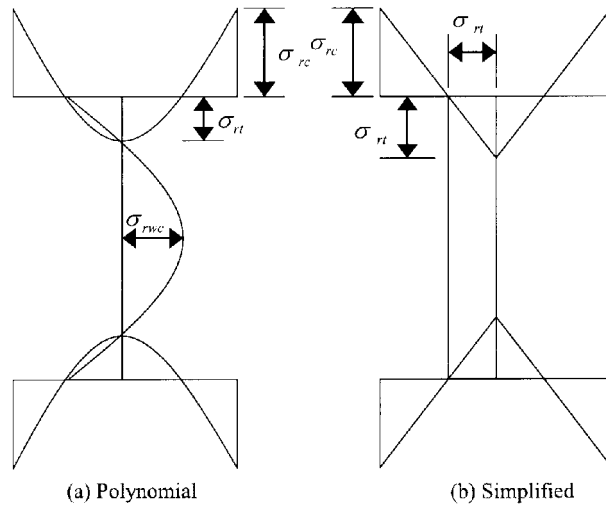


Fig. 1 Patterns of residual stresses

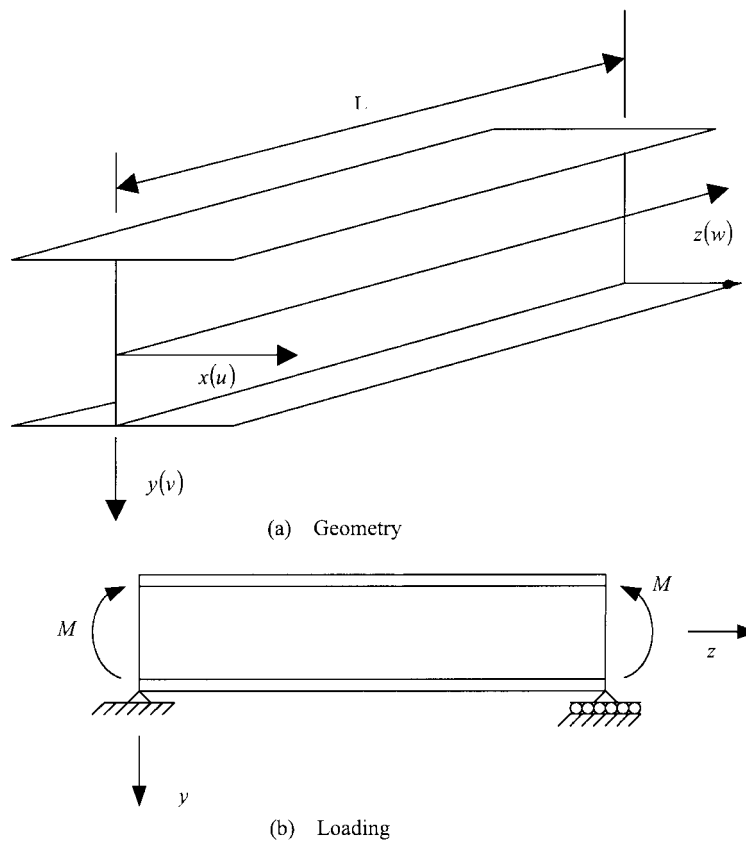


Fig. 2 Geometry and Loading

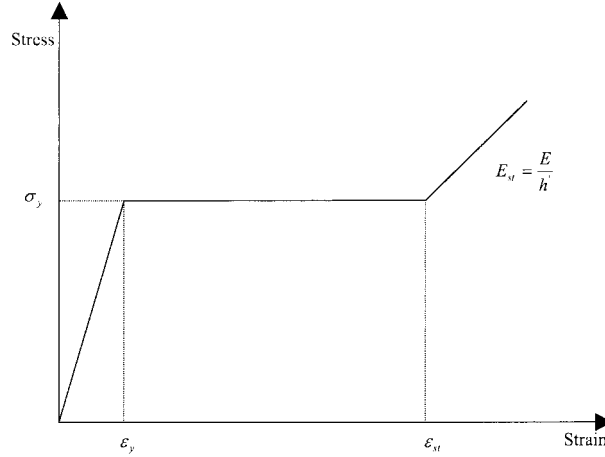


Fig. 3 Stress-strain relationship for mild steel

tapered beam-columns were simplified greatly as the terms relating to lack of coincidence of the shear centre and centroid do not appear with this model. As noted earlier, the cross-section becomes monosymmetric once yielding commences due to the presence of residual stresses.

2.2. Moment-curvature relationship

Under the action of a curvature ρ applied to the cross-section, the applied strain ϵ_a at any point in the cross-section can be found from

$$\epsilon_a(x, y) = (y + \bar{y})\rho + \epsilon_r(x, y) \quad (1)$$

where \bar{y} is the coordinate of the neutral axis relative to the web mid-height and ϵ_r is the residual strain. Fig. 3 shows the elastic-plastic-strain hardening constitutive model for the mild steel. The stress σ in the cross-section can be obtained from the applied strain in the following mathematical representation of Fig. 3.

$$\sigma(x, y) = \int_{\epsilon_r}^{\epsilon_a} E_t d\epsilon_a + E\epsilon_r \quad (2)$$

In Eq. (2), E_t is the appropriate tangent modulus (E , 0, or E_{st}) shown in Fig. 3.

The position of the neutral axis \bar{y} is dependent on the particular applied curvature ρ and must be determined iteratively. At a given value of \bar{y} , the corresponding axial force in the section N can be determined from

$$N = \int_A \sigma(x, y) dA \quad (3)$$

in which A is the area of the cross-section, and equilibrium at the cross-section dictates that N must vanish. Hence the axial force is calculated as \bar{y} is increased in steps until it changes sign. Once bracketed, the method of False Position is used to converge on the value of \bar{y} for which $N = 0$.

Finally, at the given curvature ρ for which \bar{y} is uniquely defined by equilibrium, the corresponding moment in the section M_x is simply given by

$$M_x = \int_A \sigma(x, y) y dA \quad (4)$$

The dependence of $\varepsilon_0(x, y)$ in Eq. (2) and M_x in Eq. (4) on the applied curvature ρ are used subsequently in the buckling analysis.

2.3. Buckling deformations

When the cross-section buckles out-of-plane as shown in Fig. 4, the top and bottom flanges displace laterally u_T and u_B and twist ϕ_T and ϕ_B . All of these deformations are assumed to follow the longitudinal sinusoidal eigenmode associated with lateral-torsional buckling, that is

$$\begin{Bmatrix} u_T \\ u_B \\ \phi_T \\ \phi_B \end{Bmatrix} = \begin{Bmatrix} q_1 \\ q_2 \\ q_3 \\ q_4 \end{Bmatrix} \sin \frac{n\pi z}{L} \quad (5)$$

where n is the number of harmonics into which the beam buckles and $\{q\} = q_i$ ($i = 1, \dots, 4$) are the maximum amplitudes of the buckling displacements. The web is further assumed to distort during buckling as a cubic curve, so that

$$u_w = h(1, \eta, \eta^2, \eta^3) \{\alpha\} \sin \frac{n\pi z}{L} \quad (6)$$

where $\{\alpha\}$ is a vector of four polynomial coefficients. This vector can be determined by imposing the following geometric compatibility conditions at the top and bottom flange-web junctions at $z = L/2n$:

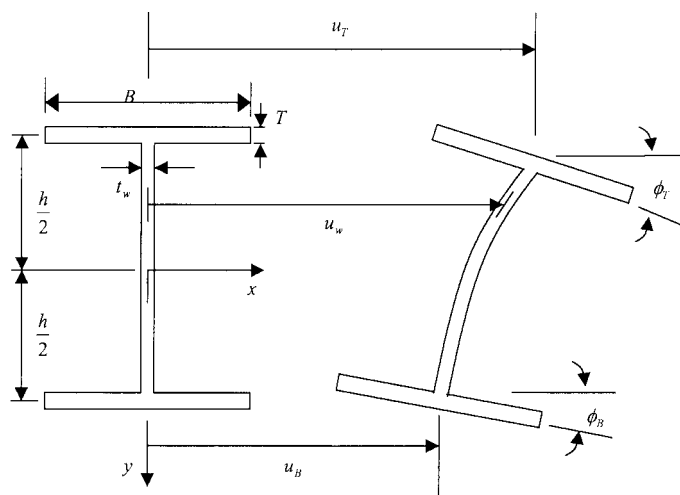


Fig. 4 Buckling deformations in the plane of the cross-section

$$u_T = (u_w)_{\eta=1/2} \quad u_B = (u_w)_{\eta=-1/2} \quad \phi_T = -(u_{w,y})_{\eta=1/2} \quad \phi_B = (u_{w,y})_{\eta=-1/2} \quad (7)$$

where commas denote partial differentiation, so that after some algebraic manipulation,

$$\{\alpha\} = \begin{bmatrix} 1/2h & 1/2h & 1/8 & -1/8 \\ 3/2h & -3/2h & 1/4 & 1/4 \\ 0 & 0 & -1/2 & 1/2 \\ -2/h & 2/h & -1 & -1 \end{bmatrix} \begin{Bmatrix} u_T \\ u_B \\ \phi_T \\ \phi_B \end{Bmatrix} \quad (8)$$

2.4. Strain energy stored during buckling

During bifurcative buckling, strain energy U is stored in the beam. This strain energy is the sum of that stored in the flanges (U_f), the web (U_w) and in the elastic restraints (U_r). The incorporation of inelasticity in this study is reliant on the infinitesimal nature of the buckling deformations, so that when incorporated in a rational model of plasticity, unloading from the yield surface is assumed to be precluded. Because of this, the inelastic model may be thought of as a quasi-elastic model, with appropriate rigidities independent of the buckling deformations.

Using this assumption, which has been used successfully for bifurcative buckling elsewhere (Dawe and Kulak 1984, Bradford 1986), the flanges are considered to be 'rigid beams' whose behaviour in the inelastic range is governed by tangent modulus theory, while the web is considered to be a plate element whose inelastic buckling behaviour is described by a constitutive matrix appropriate for the flow theory of elasticity. The strain energies stored in the flanges and in the web are then

$$U_f = \frac{1}{2} \int_0^L \{u_{T,zz}, u_{B,zz}, \phi_{T,z}, \phi_{B,z}\}^T [D_f] \{u_{T,zz}, u_{B,zz}, \phi_{T,z}, \phi_{B,z}\} dz \quad (9)$$

$$U_w = \frac{1}{2} \int_0^L \{u_{w,yy}, u_{w,zz}, -2u_{w,yz}\}^T [D_w] \{u_{w,yy}, u_{w,zz}, -2u_{w,yz}\} dydz \quad (10)$$

where the property matrices for the flanges and web respectively are

$$[D_f] = [(EI_T), (EI_B), (GJ_T), (GJ_B)_t] \quad (11)$$

$$[D_w] = \begin{bmatrix} w_1 & w_2 & 0 \\ w_2 & w_3 & 0 \\ 0 & 0 & w_4 \end{bmatrix} \quad (12)$$

In Eq. (11), the tangent modulus theory model Trahair and Kitipornchai (1972) has been used to determine the minor axis flexural rigidities $(EI)_t$. This was achieved by transforming the thickness of the flanges according to a modular ratio of unity when $\varepsilon_u < \varepsilon_y$, and to $E_{sl}/E (=1/h)$ when $\varepsilon_u \geq \varepsilon_y$. This approach is based on the well-known dislocation theory of yielding. The torsional rigidities $(GJ)_t$ were calculated in the same fashion as that described in the bimetallic representation of Booker and Kitipornchai (1971). While the formulation of the polynomial residual stress distribution stated by Bradford and Trahair (1985) satisfies the static and torsional equilibrium conditions.

$$\int_A \sigma_r dA = \int_A (x^2 + y^2) dA = 0 \quad (13)$$

accepted models of simplified residual stress distributions do not. Because of this, it is necessary to alter the tangent torsional rigidity in Eq. (11) to

$$(GJ)_t - \int_A \sigma_r (x^2 + y^2) dA$$

in order to eliminate the unequilibrating axial torque induced by the residual stresses, which is related to the Wagner effect (Trahair 1993).

In the web property matrix in Eq. (12), the entries w_i were determined from the usual isotropic elastic theory of Timoshenko and Woinowsky-Krieger (1959) at positions y in the cross-section where $\epsilon_a < \epsilon_y$. For those positions y where $\epsilon_a > \epsilon_y$, the model of Haaijer (1957) which was adopted and verified experimentally by Dawe and Kulak (1984) and Bradford (1986) was used. In this representation,

$$w_1 = \frac{E_{st} t_w^3}{12[1 - (v_1 v_2)]} \quad w_2 = w_3 = 2 \frac{E_{st} t_w^3}{12[1 - (v_1 v_2)]} \frac{(2v - 1)E_{st} + E}{3E_{st} + E} \quad w_4 = \frac{G_{st} t_w^3}{12} \quad (14)$$

where

$$(v_1 v_2) = \frac{[(2v - 1)E_{st} + E]^2}{E(3E_{st} + E)} \quad (15)$$

and v is the elastic Poisson's ratio (taken as 0.3 herein).

The continuous elastic restraints that may inhibit lateral deformation, lateral rotation and twist rotation at the top and bottom flanges are the same as those described by Bradford (1988a). These restraints are depicted in Fig. 5. If the vectors $\{r\}$ and $\{\epsilon_r\}$ represent the conjugate (infinitesimal) restraining actions and deformations respectively, then,

$$U_r = \frac{1}{2} \int_0^L \{r\}^T \{\epsilon_r\} dz = \frac{1}{2} \int_0^L \{\epsilon_r\}^T [k_r] \{\epsilon_r\} dz \quad (16)$$

where $[k_r]$ is the elastic continuous restraint stiffness matrix.

The generalised strain terms in Eqs. (9), (10) and (16) may be obtained by appropriate differentiation of Eqs. (5) and (6). When this differentiation is performed, the strain energies may be written as

$$U_f = \frac{1}{2} \{q\}^T [K_f] \{q\}, \quad U_w = \frac{1}{2} \{q\}^T [K_w] \{q\}, \quad U_r = \frac{1}{2} \{q\}^T [K_r] \{q\} \quad (17)$$

and the total strain energy stored during buckling as

$$U = \frac{1}{2} \{q\}^T [K] \{q\} \quad (18)$$

where $[K_r]$ is the (constant) elastic restraint stiffness matrix, and $[K_f]$ and $[K_w]$ are the flange and web stiffness matrices respectively, whose entries depend on the level of applied loading.

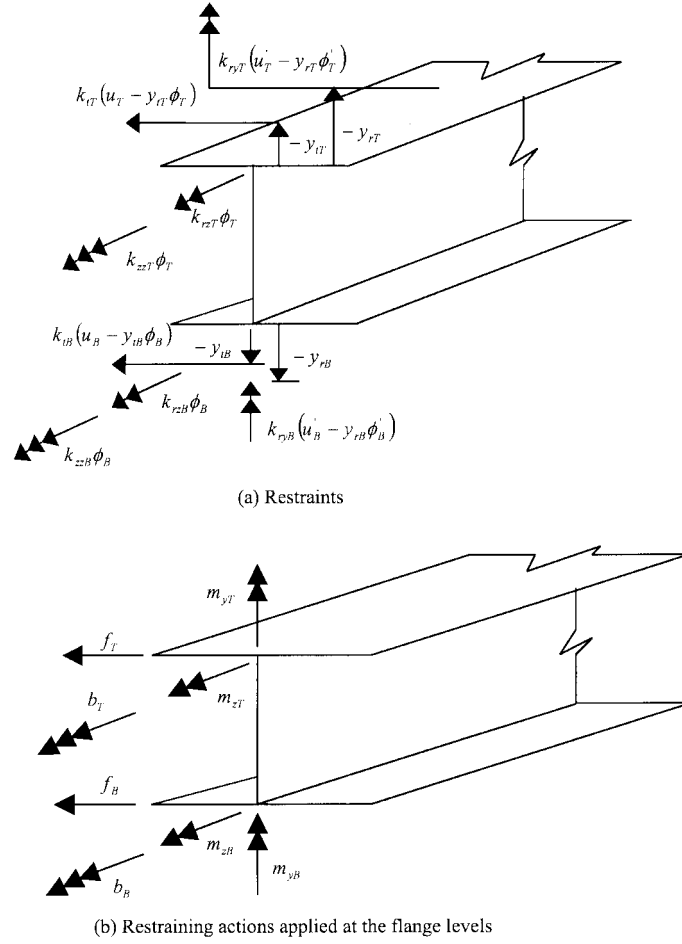


Fig. 5 Elastic restraints

2.5. Work done during buckling

The loss of potential during buckling caused by the applied moment λM is the sum of the contributions for the flanges and web. Thus,

$$V = V_f + V_w \quad (19)$$

where

$$V_f = \frac{1}{2} \int_{A_f} \lambda \sigma \int_0^L (u_{T,z}^2 + u_{B,z}^2 + x^2 \phi_{T,z}^2 + x^2 \phi_{B,z}^2) dz dA_f \quad (20)$$

$$V_w = \frac{1}{2} \int_{A_w} \lambda \sigma \int_0^L u_{w,z}^2 dz dA_w \quad (21)$$

in which

$$\lambda\sigma = \frac{\lambda M_y}{I_x} \quad (22)$$

and A_f and A_w are the flange and web areas respectively. The derivatives in Eqs. (20) and (21) may be obtained from Eqs. (5) and (6), so that the former equations may be written as

$$V_f = \frac{1}{2}\{q\}^T [S_f] \{q\}, \quad V_w = \frac{1}{2}\{q\}^T [S_w] \{q\} \quad (23)$$

and the total work done during buckling as

$$V = \frac{1}{2}\{q\}^T [S] \{q\} \quad (24)$$

where $[S_f]$ and $[S_w]$ are the flange and web stability matrices respectively, and whose entries depend on the level of applied loading.

2.6. Bifurcation of equilibrium

The total change in potential Π can be written as

$$\Pi = U - V = \frac{1}{2}\{q\}^T [A(\lambda)] \{q\} \quad (25)$$

where the 4×4 matrix $[A] = [K] - [S]$ depends on the level of loading λ . Since $[A]$ has been derived in terms of the deformations of the secondary equilibrium path $\{q\}$ that are departures from the (trivial) primary equilibrium path at the point of bifurcation, this point may be located by invoking the equilibrium condition in variational form that

$$\delta\Pi = \{\delta q\}^T [A] \{q\} = 0 \quad (26)$$

for any arbitrary perturbation $\{\delta q\}$. Hence from Eq. (26), the 4th order eigenproblem

$$[A]\{q\} = \{0\} \quad (27)$$

can be established.

In the solution of Eq. (27), the method used by Smith *et al.* (2000) has been modified for the problem at hand. This involves the specification of a reference moment level M , and the application of a monotonic load factor λ to M . For a particular moment λM , the corresponding curvature is invoked from the predetermined moment-curvature response, and the matrix $[A]$ can be assembled. This matrix is then reduced simply to upper triangular form by Gaussian elimination without row interchanges, and the determinant is calculated by multiplying the four diagonals of the reduced matrix. The number of eigenvalues less than the trial loading level specified by λ is given by the number of negative diagonal elements in the reduced matrix, and the load level for which this number is unity is sought. Once the monotonic increment on λ brackets the lowest eigenvalue, the method of bisections is used to converge on the critical value of the load factor to a predetermined tolerance. At this value of λ_{cr} , the corresponding eigenvector $\{q\}$ in Eq. (27) can be determined.

3. Accuracy of solution

Since inelastic lateral-torsional buckling results for hot-rolled I-section beams are fairly well established and accepted, in deference to lateral-distortional buckling, the results with cross-sectional distortion suppressed have been compared with the lateral-torsional buckling predictions reported by Trahair and Kitipornchai (1972). The beam considered in this study was the widely-used 8WF31, whose geometric and material properties are given in Fig. 6. The residual stresses used in the study herein were the polynomial pattern recommended by Lee *et al.* (1967) and the simplified pattern specified by Trahair and Kitipornchai (1972). So that the lateral-distortional buckling model developed herein can be compared with the lateral-distortional buckling results reported in the literature, the effect of web plate flexure during buckling must be eliminated. This may be achieved by identifying the term

$$\frac{1}{2} \int_0^L \int_{-h/2}^{h/2} w_1 u_{w,yy}^2 dy dz$$

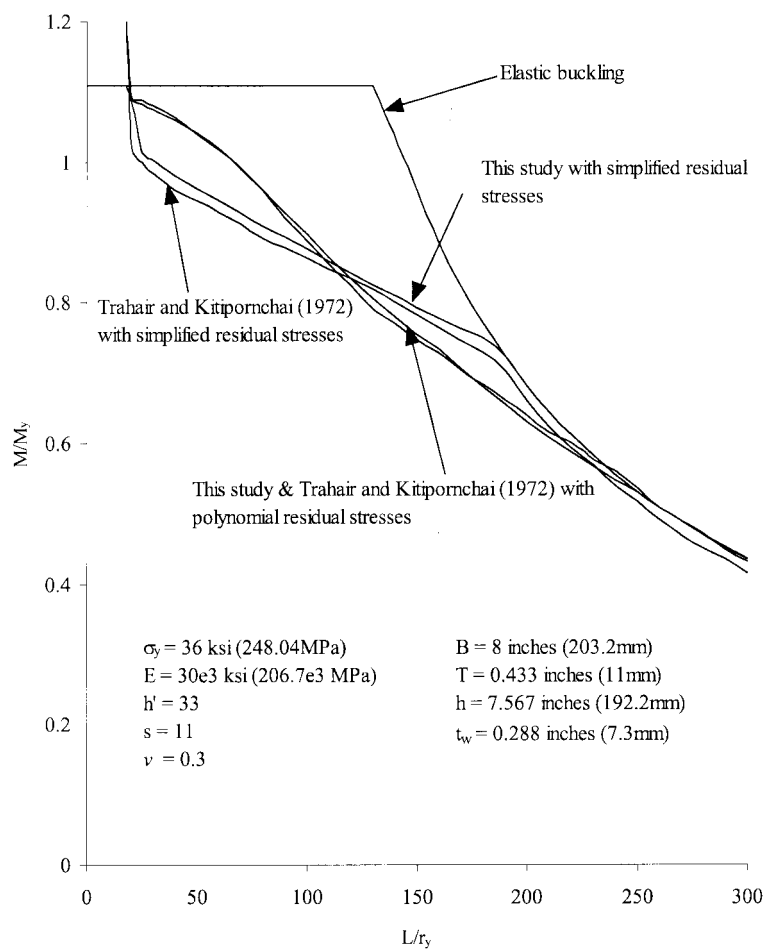


Fig. 6 Inelastic lateral-torsional buckling of unrestrained beam in uniform bending

in Eq. (10), and scaling it by a large number (10^8 was used here).

Fig. 6 shows the comparison between the model reported herein and the results of Trahair and Kitipornchai (1972). It can be seen that the results are almost in complete agreement for the polynomial residual stress pattern, but that there is a small discrepancy between the two methods for the simplified residual stress pattern. This discrepancy appears to be a result of the inability of Trahair and Kitipornchai's model to enforce complete torsional equilibrium, as is indicated by their solution lying slightly above the theoretical elastic solution as the elastic range of response is entered. As would be expected, the influence of the model of residual stress does not affect the value of the beam slenderness L/r_y at which strain-hardening buckling takes place, and the results of both investigations are in agreement when the buckling moment equals the plastic moment of resistance.

4. Inelastic buckling of an unrestrained beam

A number of studies reported in the literature have indicated that the inelastic lateral-torsional buckling moment for an unrestrained I-beam has a profound dependence on the model of the residual stresses. This influence of the residual stresses results from their dependence on the geometric proportions of the beam cross-section, and the simplified model was used in the current method to study the inelastic lateral-distortional buckling of four different cross-section types: 610UB113 and 360UB50.7 universal beam sections manufactured in Australia, and an 8WF31 and Australian 310UC118 universal column sections. The material properties used were: $E = 200$ GPa, $\sigma_y = 250$ MPa, $\nu = 0.3$, $\epsilon_s/\epsilon_y = 10$ and $h' = 33$.

The results of the inelastic buckling study are shown in Fig. 7, where they are compared with the corresponding results reported by Bradford and Trahair (1985) who analysed the same four cross-sections. The inelastic buckling moment has been normalised with respect to the full plastic moment M_p and the beam slenderness represented as $\sqrt{M_p/M_o}$, where M_o is the elastic lateral buckling moment. The disparity between the results produced by the method of this paper and that of Bradford and Trahair arises primarily because the former study uses the simplified model of residual stresses, while the latter study uses a polynomial pattern.

For design, it is necessary that the scatter of results be accounted for, at least in a conservative fashion. The predictions of the beam strength curve of the Australian AS4100 steel structures standard (SA, 1998) based on the limit state of lateral buckling are also shown in Fig. 7, and this beam curve incorporates the effects of geometric imperfections that are not included in either the Bradford and Trahair (1985) model, or the method developed herein. Generally, the AS4100 curve is quite conservative, except for stocky beams. This unconservatism has also been noted elsewhere (Trahair 1993, Trahair and Bradford 1998), but it should be noted that neither method includes the benign effect of major axis bending curvature (Trahair 1993).

5. Inelastic distortional buckling of an elastically restrained beam

5.1. General

The effect of continuous elastic restraints on the inelastic buckling of I-section beams has been investigated. In this study, the cross-sections considered in the previous section with the simplified model of residual stresses were adopted, with the beam subjected to continuous translational, minor axis rotational and

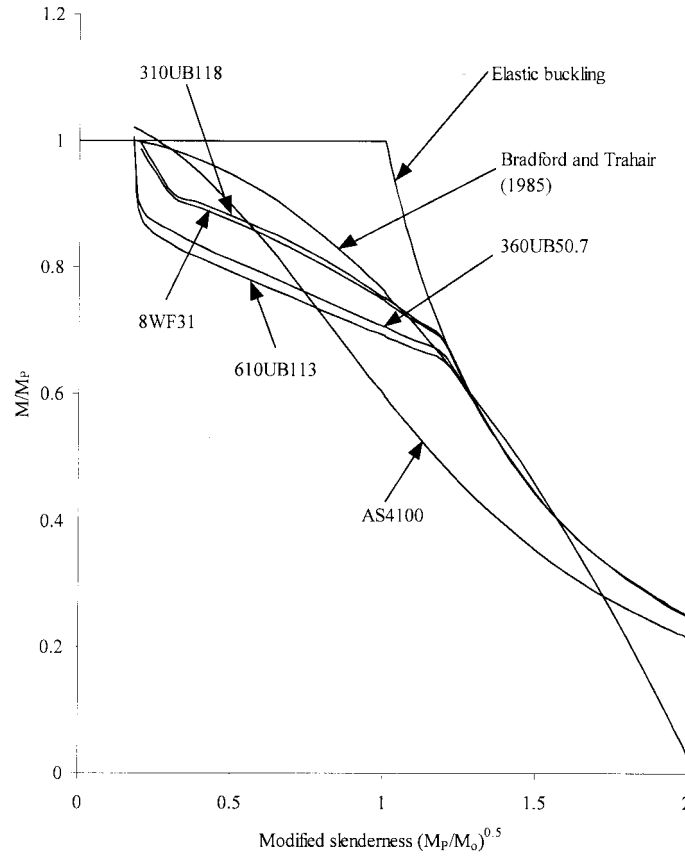


Fig. 7 Inelastic lateral-torsional buckling results

twist rotational (torsional) restraints applied at the tension flange level. The stiffness of the translational restraint per unit length is k_t , the minor axis restraint stiffness per unit length is k_{ry} , and the torsional restraint is k_z , and these have been expressed in the non-dimensional form (Trahair 1979, Bradford 1988a).

$$\alpha_t = \frac{k_t L^2}{\pi^2 N_y} \alpha_{ry} = \frac{k_{ry}}{N_y} \alpha_z = \frac{k_z L^2}{\pi^2 GJ} \quad (28)$$

where N_y is the Euler load, and GJ is the elastic Saint Venant torsional rigidity.

The lateral-torsional buckling moments have also been calculated in this study in order to compare them with those of the lateral-distortional buckling analysis by modifying the rigidity of the web in the same fashion as described earlier. In the graphs generated in the investigation, the dimensionless buckling moment M/M_y has been plotted as a function of the dimensionless beam length L/h , where M_y is the first-yield moment of the cross-section in the absence of residual stresses.

5.2. Minor axis rotational restraint

In this study, 360UB50.7 and 310UC118 cross-sections were considered, and the continuous minor axis rotational restraint of dimensionless stiffness α_{ry} was applied at the tension flange level. The results

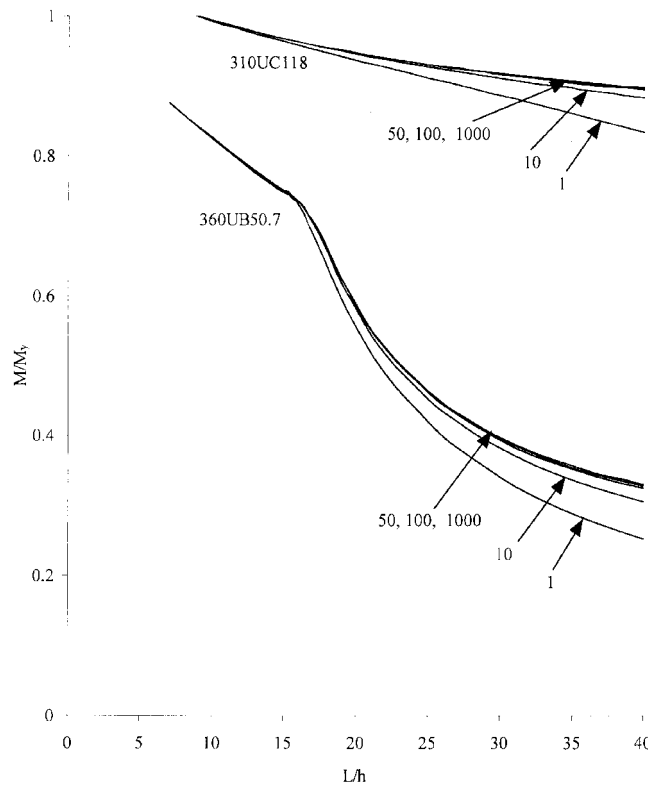


Fig. 8 Inelastic buckling of beam with minor axis rotational restraint

are shown in Fig. 8, where it can be seen that increases in the stiffness of the elastic restraint increase the buckling moment for longer beam lengths, but the effect being only minor with decreased beam lengths for which buckling is accompanied by significant yielding. The inelastic lateral-distortional and inelastic lateral-torsional buckling moments virtually coincide, indicating that the buckling is not accompanied by distortion of the cross-section.

5.3. Translational restraint

A similar investigation has been carried out on 360UB50.7 and 310UC118 cross-sections with continuous translational restraint of non-dimensionalised stiffness α_t . It was found that the results are identical to those presented in Fig. 8, but with k_{ry} replaced with $k_t L^2 / \pi^2 N_y$. This result was proven for elastic lateral-torsional buckling by Trahair (1979), and shown to be true for elastic lateral-distortional buckling by Bradford (1988a). Fig. 9 shows additional results for 610UB113 and 8WF31 cross-sections, and for which a similar conclusion can be made regarding the duality of the continuous minor axis and translational buckling restraints.

5.4. Torsional restraint

It was shown by Bradford (1988a) that cross-sectional distortion has a profound effect on the elastic

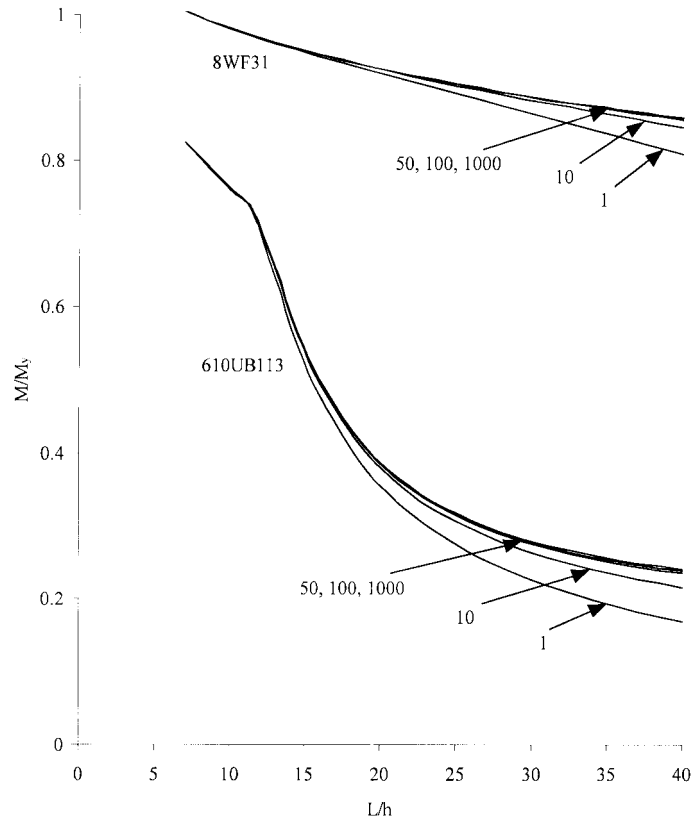


Fig. 9 Inelastic buckling of beam with translational restraint

distortional buckling load of a beam with complete continuous and elastic torsional restraint against buckling applied at the level of the tension flange. It was shown further that while the assumptions of Vlasov theory upon which the predictions of Trahair (1979) were based predict an infinite buckling moment as α_z increases towards infinity, the relaxing of the assumption of cross-sectional rigidity leads to finite elastic buckling moments. The extension of this conclusion into inelastic buckling, in which the full plastic moment with strain hardening neglected was argued to be an upper bound on the beam strength (Bradford 2000), has been considered in more detail here with a 610UB113 cross-section and the well-researched 8WF31 cross-section.

The buckling results are shown in Fig. 10. At low values of α_z ($=1$), the beam with a 610UB113 cross-section was found to buckle into one harmonic ($n=1$) irrespective of length. However, in the range $10 \leq \alpha_z \leq 100$ the lowest value of the buckling moment did not correspond to the fundamental mode, and the number of harmonics required to produce the lowest inelastic buckling moment was dependent on the beam length. For instance, with $\alpha_z = 10$ the beam was found to buckle in the fundamental mode ($n=1$) for $L/h > 14.5$ approximately, but with $n=2$ for dimensionless lengths less than this value. This limiting value is shown in Fig. 10. Further, with $\alpha_z = 50$ the beams buckle with two harmonics ($n=2$) for $L/h > 40$ approximately, with three harmonics ($n=3$) for $30 < L/h < 40$ approximately, with four harmonics ($n=4$) for $17 < L/h < 40$ approximately, and with five harmonics ($n=5$) for $10 < L/h < 17$ approximately. For values of the dimensionless lengths less than 10, the number

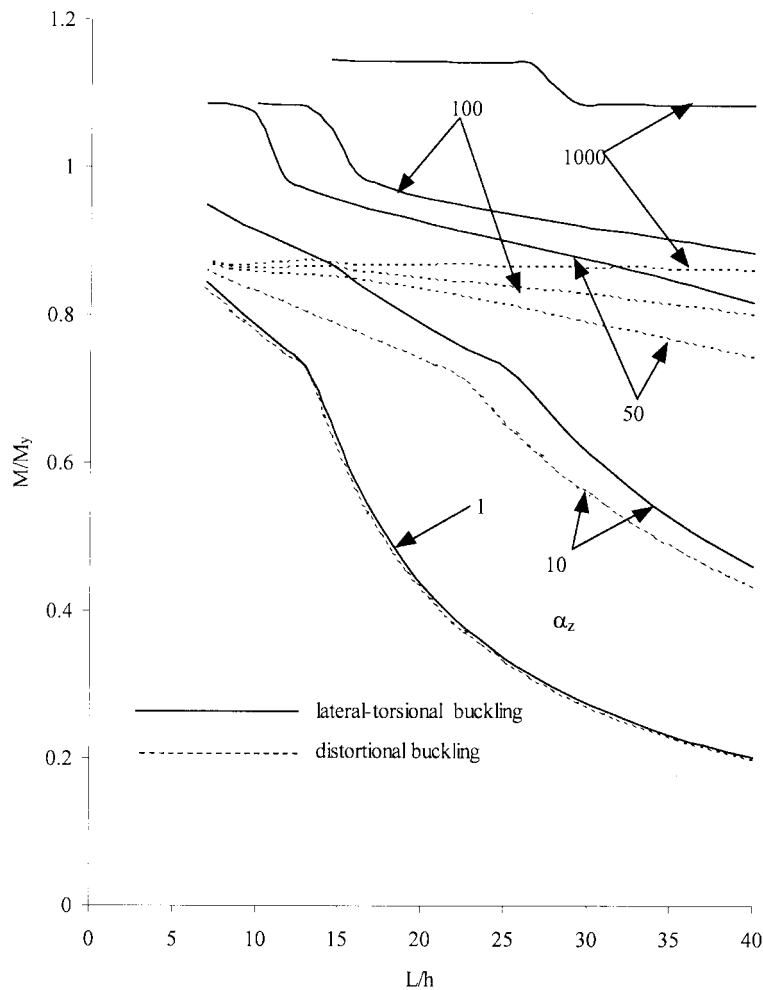


Fig. 10 Inelastic buckling of deep 610UB113 with torsional restraint

of harmonics needed to achieve the lowest buckling load was found to decrease, but in this length range the buckling mode is inelastic local, and cannot be predicted accurately by the distortional buckling method of this paper. Similar trends for the 610UB113 cross-section were found for $\alpha_z = 100$ and 1000.

Corresponding buckling curves have been obtained for the stockier wide-flange 8WF31 profile, and these are given in Fig. 11. Unlike the narrower 610UB profile, the wide flange profile was found to buckle with four harmonics ($n = 4$) for $L/h > 30$ approximately, but progressively decreasing to two harmonics ($n = 2$) as L/h decreases to about 10 which is a suitable cutoff for the occurrence of local buckling. The observation of the sometimes-high number of harmonics in the eigenmode that corresponds to the lowest eigenvalue is important in the modelling of the problem with line-type finite elements. For example, in the study reported by Bradford (2000), eight equal-length elements were used, but reducing this number of elements (which use cubic interpolation polynomials) may cause inaccuracies in the solution if the number of harmonics is large.

Figs. 10 and 11 also show the results obtained for inelastic lateral-torsional buckling. It can be seen

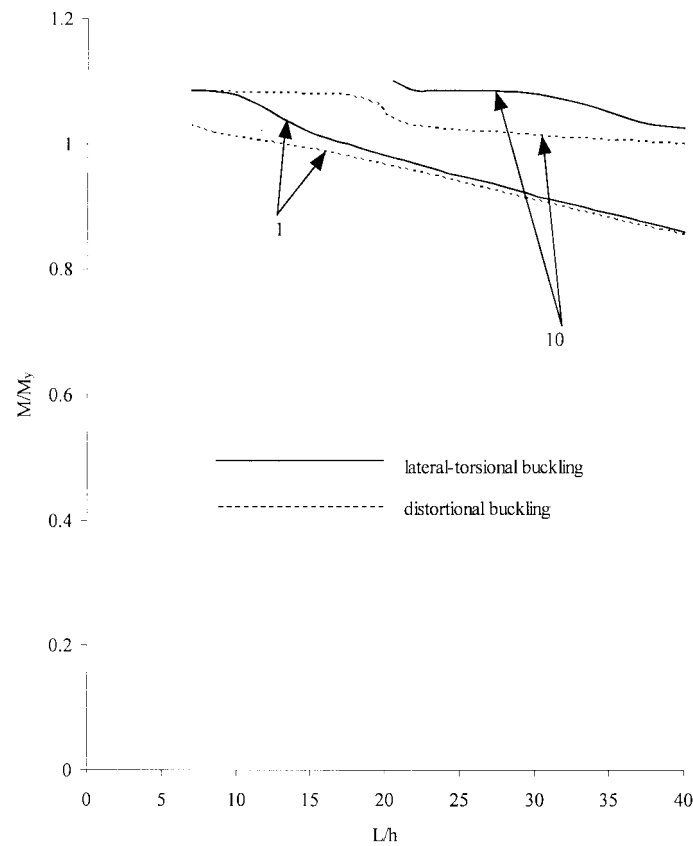


Fig. 11 Inelastic buckling of wide 8WF31 with torsional restraint

that as a_z is increased the lateral-torsional and lateral-distortional results become increasingly disparate, with the former being unconservative. This trend occurs even for shorter beam-lengths for which buckling occurs with highly inelastic cross-sections, and the lateral-torsional buckling results occur in the strain hardening range of material behaviour.

6. Conclusions

This paper has considered the inelastic lateral-distortional buckling of an I-section beam under uniform bending with and without continuous elastic restraints that inhibit the buckling. The method uses a quite simple harmonic representation of the eigenmode, and incorporates both the so-called simplified and polynomial patterns of residual stresses, so as to shed light on some of the important parameters that affect the buckling strength. By a simple modification of the buckling model, the results have been validated against results reported for inelastic lateral-torsional buckling that does not involve distortion of the cross-section during buckling.

For unrestrained beams with hot-rolled cross-sections (to which the study has been restricted), the buckling mode is sensibly lateral-torsional and the effects of cross-sectional distortion can be ignored.

Because of this, codified design rules for inelastic lateral-torsional buckling may be used. For beams with translational and minor axis rotational restraint, but for which the beam is free to twist during buckling, the inelastic buckling load is again very similar to that for lateral-torsional buckling. However, when restraint against twist rotation is applied to the cross-section along the beam length, the member is not free to twist during buckling and cross-sectional distortion must necessarily accompany the buckling deformation. This effect is difficult to quantify, and depends on such factors as the topology of the cross-sectional profile, the level of residual stress, the beam length and the stiffness of the torsional restraint. While the buckling strength increases with increasing stiffness of the torsional restraint when based on either a lateral-torsional or lateral-distortional modelling, the use of the latter more rational analysis leads to lower strengths than those obtained using a lateral-torsional representation. Since the fully plastic moment can only be used as an upper bound, which is not necessarily close to the predicted strength with continuous torsional restraint, care should be exercised in the use of codified design rules to model this quite common situation of beam restraint.

The many buckling half-wavelengths into which a beam may buckle has been demonstrated in the paper. This has ramifications on the use of line type finite elements for an “overall” buckling mode, since the lengthwise interpolation polynomials used in these would be at odds with predicting accurately a buckling mode that is accompanied by a large number of half wavelengths, unless a sufficiently large number of elements was chosen. The possibility of the buckling mode containing many half-wavelengths is not known initially, and the results in this paper provide greater clarity in the guidance on certain geometries where the use of line-type elements may lead to aberrations in the accuracy of the solution.

Acknowledgment

The work reported in this paper was supported in part by the Australian Research Council.

References

- Booker, J.R. and Kitipornchai, S. (1971). “Torsion of multilayered rectangular sections”, *J. Eng. Mech. Division, ASCE*, **97**(EM5), 1451-1468.
- Bradford, M.A. (1986). “Local buckling analysis of composite beams”, *Civil Engineering Transactions, I.E. Australia*, **CE28**(4), 312-317.
- Bradford, M.A. (1988a). “Buckling of elastically restrained beams with web distortions”, *Thin-Walled Structures*, **6**, 287-304.
- Bradford, M.A. (1988b). “Buckling strength of deformable monosymmetric I-beams”, *Engineering Structures*, **10**, 167-173.
- Bradford, M.A. (1990). “Design of beams with partial end restraint”, *Proceedings, Institution of Civil Engineers, London*, Part 2, **89**, 163-181.
- Bradford, M.A. (1992). “Lateral-distortional buckling of steel I-section members”, *J. Constr. Steel Res.*, **23**, 97-116.
- Bradford, M.A. (2000). “Strength of compact steel beams with partial restraint”, *J. Constr. Steel Res.*, **53**(2), 183-200.
- Bradford, M.A. and Cuk, P.E. (1988). “Lateral buckling of tapered monosymmetric I-beams”, *J. Struct. Eng., ASCE*, **114**(5), 977-996.
- Bradford, M.A. and Trahair, N.S. (1981). “Distortional buckling of I-beams”, *J. Structural Division, ASCE*,

- 107(ST2), 355-370.
- Bradford, M.A. and Trahair, N.S. (1983). "Lateral stability of I-beams on seats", *J. Structural Eng.*, ASCE, **109**(9), 2212-2215.
- Bradford, M.A. and Trahair, N.S. (1985). "Inelastic buckling of beam-columns with unequal end moments", *J. Constr. Steel Res.*, **5**, 195-212.
- Dawe, J.L. and Kulak, G.L. (1984). "Plate instability of W shapes", *J. Struct. Eng.*, ASCE, **110**(6), 1278-1291.
- Galambos, T.V. (1963). "Inelastic lateral buckling of beams", *J. Struct. Div.*, ASCE, **89**(ST5), 217-242.
- Haaijer, G. (1957). "Plate buckling in the strain-hardening range", *J. Eng. Mechanics Division*, ASCE, **83**(EM2), 1212-1247.
- Ketter, R.L., Kaminsky, E.L. and Beedle, L.S. (1955). "Plastic deformation of wide-flange beam-columns," *Transactions*, ASCE, **100**, 1028-1061.
- Kitipornchai, S. and Trahair, N.S. (1975). "Inelastic buckling of simply supported steel I-beams", *J. Struct. Div.*, ASCE, **101**(ST7), 1333-1347.
- Lee, D-S and Bradford, M.A. (2002). "Inelastic distortional buckling of simply supported beams by the finite element method," submitted for publication.
- Lee, G.C., Fine, D.S. and Hastrieter, W.R. (1967). "Inelastic torsional buckling of H-columns", *J. Structural Division*, ASCE, **93**(ST5), 295-307.
- Nethercot, D.A. (1974). "Residual stresses and their influence upon the lateral buckling of rolled steel beams", *The Structural Engineer*, **52**(3), 89-96.
- Smith, S.T., Bradford, M.A. and Oehlers, D.J. (2002). "Inelastic unilateral buckling of mild steel plates using a Ritz-based method", *Int. J. Num. Methods in Eng.*, (to appear).
- Standards Australia (1998). *AS4100 steel structures*, S.A., Sydney, Australia.
- Timoshenko, S.P. and Woinowsky-Krieger, S. (1959). *Theory of Plates and Shells*, McGraw Hill, New York.
- Trahair, N.S. (1979). "Elastic lateral buckling of continuously restrained beam-columns", in *The Profession of a Civil Engineer* (E.H. Davis and D. Campbell-Allen, eds.), Sydney University Press, Sydney, Australia, 61-73.
- Trahair, N.S. (1993). *Flexural-Torsional Buckling of Structures*. E&FN Spon, London.
- Trahair, N.S. and Kitipornchai, S. (1972). "Buckling of inelastic I-beams under uniform moment", *J. Struct. Div.*, ASCE, **98**(ST11), 2551-2566.
- Trahair, N.S. and Bradford, M.A. (1998). *The behaviour and design of steel structures to AS4100*, 3rd Australian edn., E&FN Spon, London.